

## Electronic Supplementary Information (ESI)

### Design of bi-functional oxide electrode for selective oxidative C-C cleavage of glycerol to Formic acid and synchronized green hydrogen production

Arindam Saha,<sup>a,b</sup> Vasantharadevi Murugiah,<sup>a</sup> Ravi Ranjan,<sup>a,b</sup> Inderjeet Chauhan,<sup>a,b</sup> Kshirodra Kumar Patra,<sup>a</sup> Himanshu Bajpai,<sup>a</sup> Avisekh Saha,<sup>a,b</sup> Chinnakonda S Gopinath<sup>a,b,\*</sup>

<sup>a</sup>Catalysis and Inorganic Chemistry Division, CSIR-National Chemical Laboratory, Dr. Homi Bhabha Road, Pune 411 008, India.

<sup>b</sup>Academy of Scientific and Innovative Research (AcSIR), Ghaziabad 201002, India.

\*Corresponding author. E-mail: [cs.gopinath@ncl.res.in](mailto:cs.gopinath@ncl.res.in)

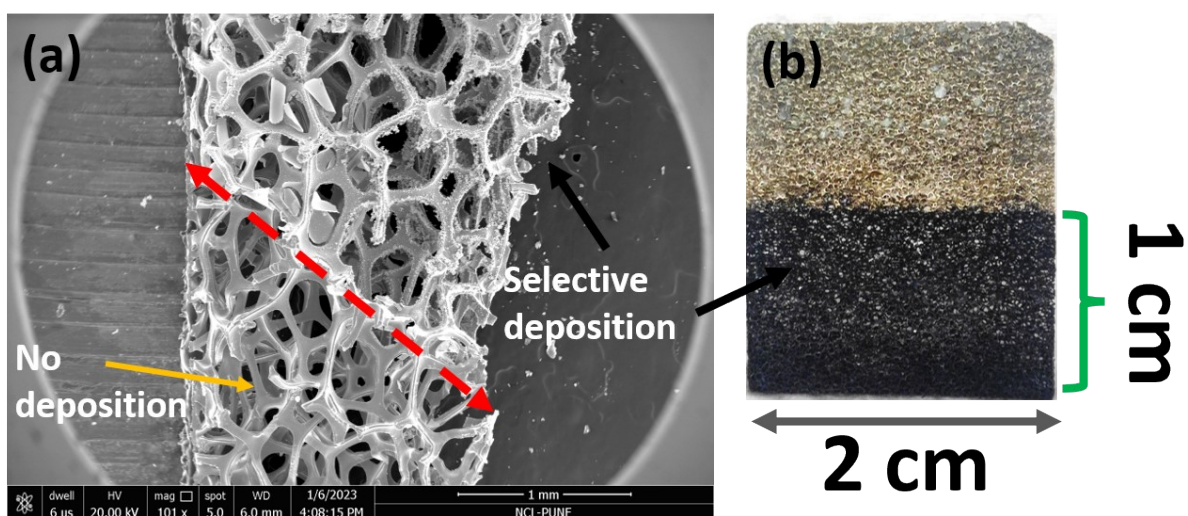


**Fig. S1** (a) Low-resolution FESEM image of catalyst coated on Ni-foam. (b) Selective deposition of the catalyst precursor after hydrothermal synthesis. Top 1x2 cm<sup>2</sup> was covered with teflon and avoided catalyst deposition.

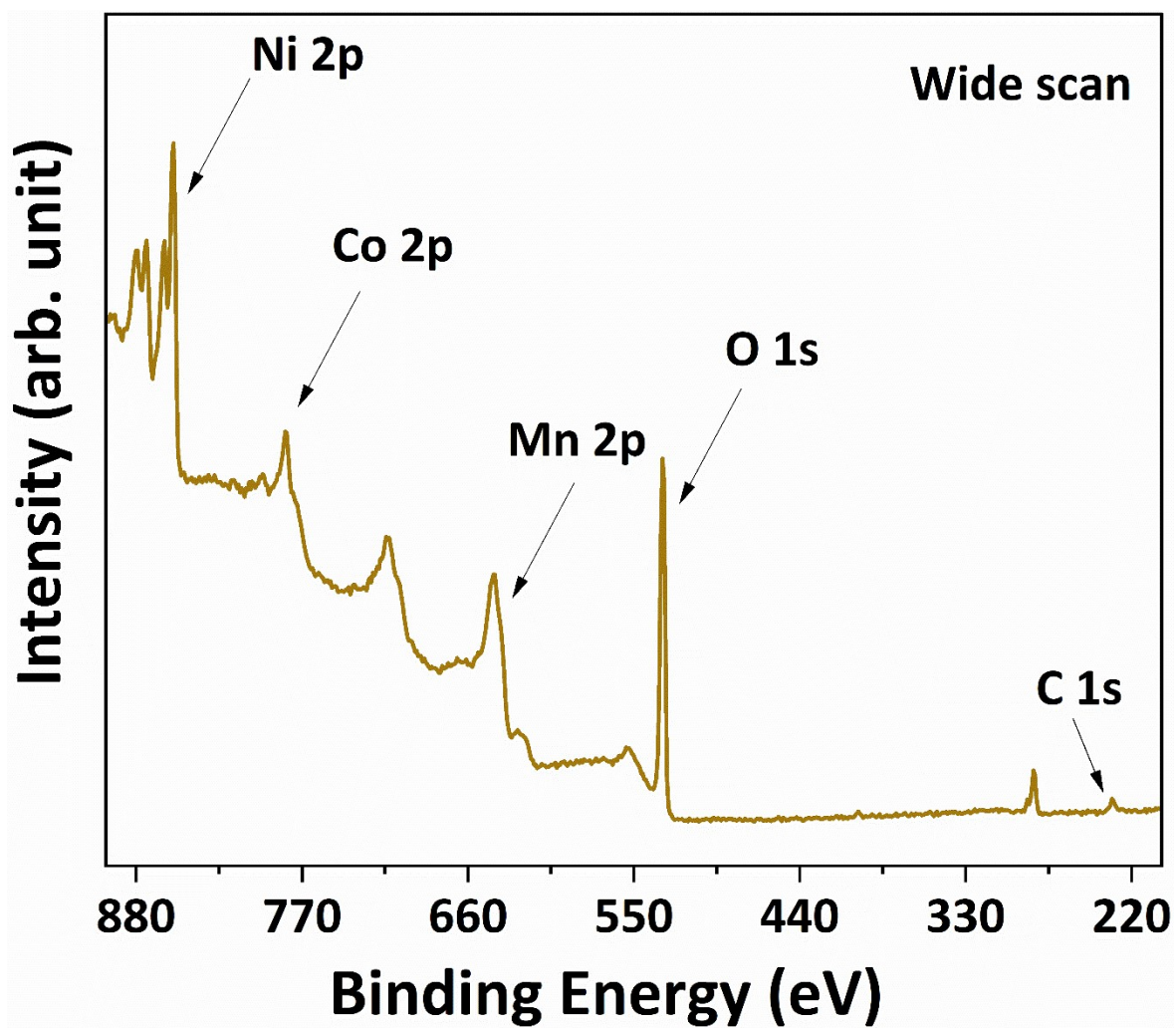


**Fig. S2** Wide Scan XPS spectra of NCMO/NF. This shows the presence of all the three metal-ions (Ni, Co, Mn) along with oxygen.

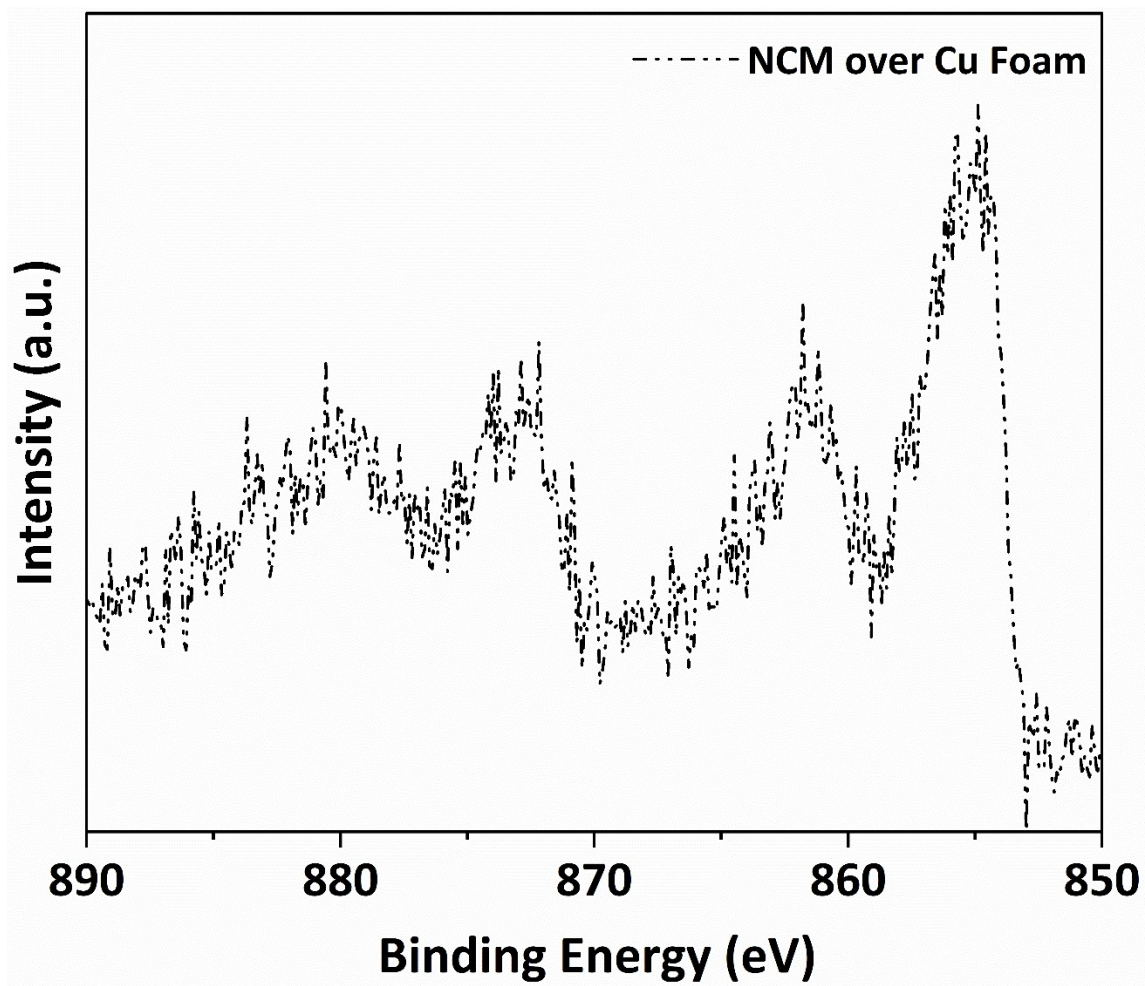


**Fig. S3** NiCoMn oxide deposited over Cu Foam to eliminate the metallic Ni peak in XPS spectra

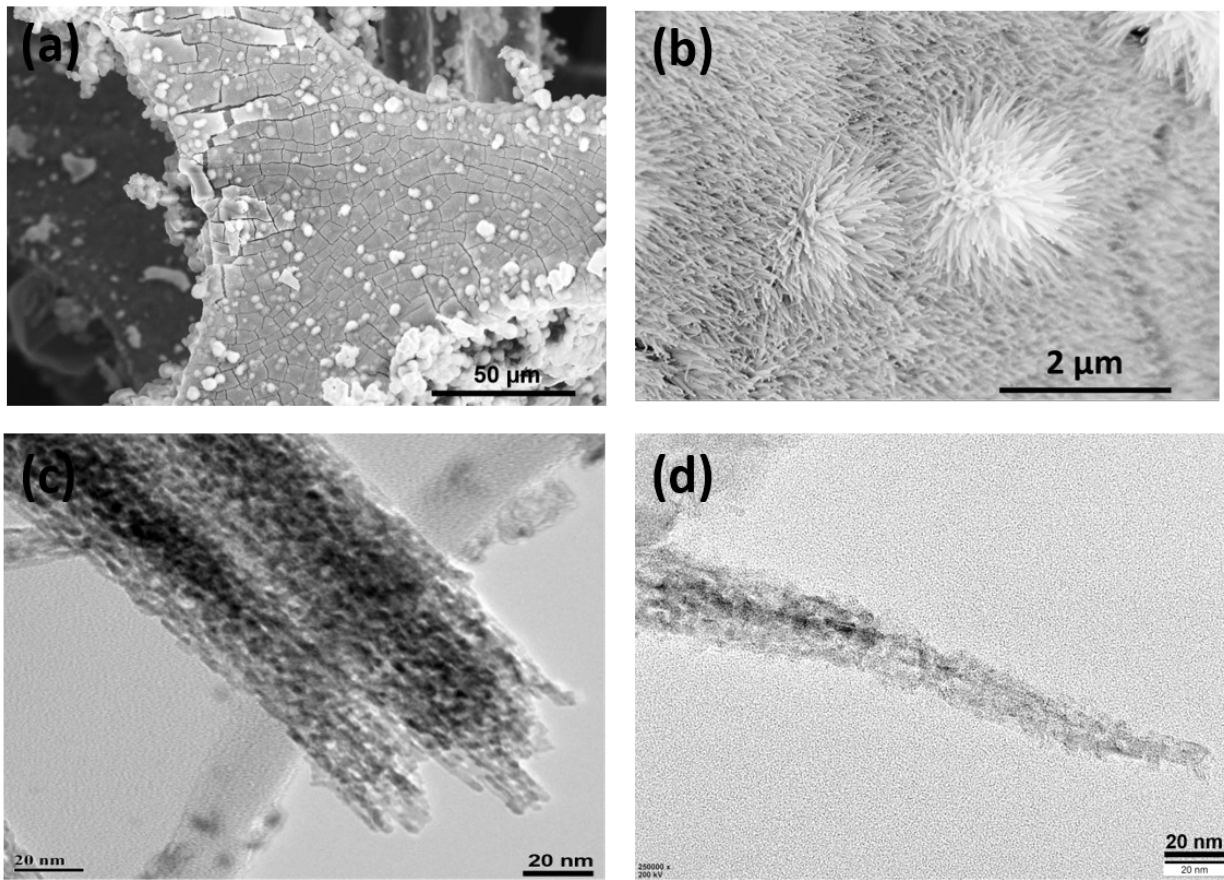


**Fig. S4** (a) Distribution of nanoneedle over NF-ligament. (b) Lateral view of growing nanoneedle and accumulative cactus structure (c) Pores present in the (c) bunch of nanoneedles, and (d) an isolated nanoneedle.



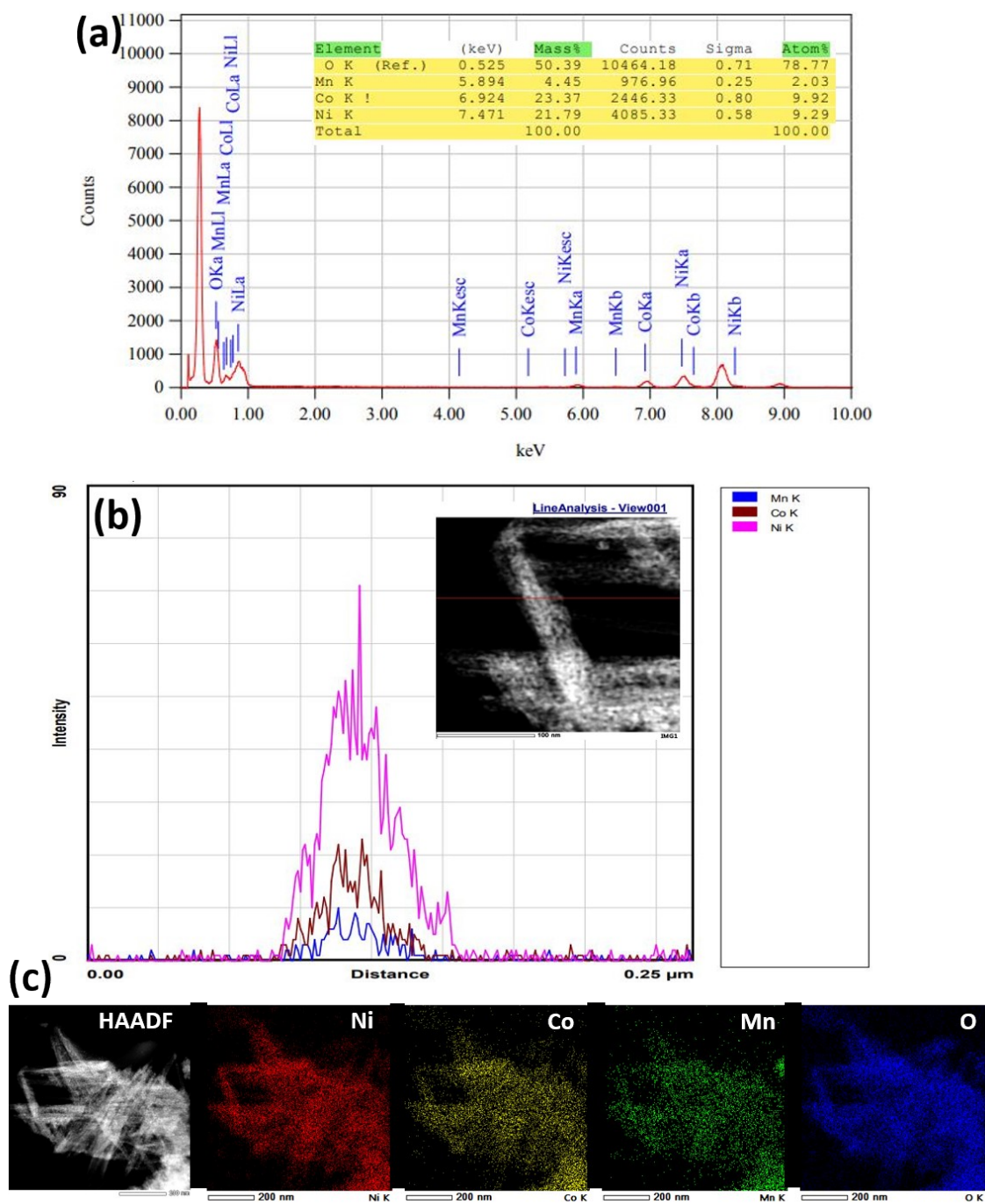


**Fig. S5** (a) Energy dispersive x-ray analysis for the quantification of all elements. (b) Line profile analysis of metals on isolated nanoneedle. (c) Elemental mapping on a set of aggregated nanoneedle.

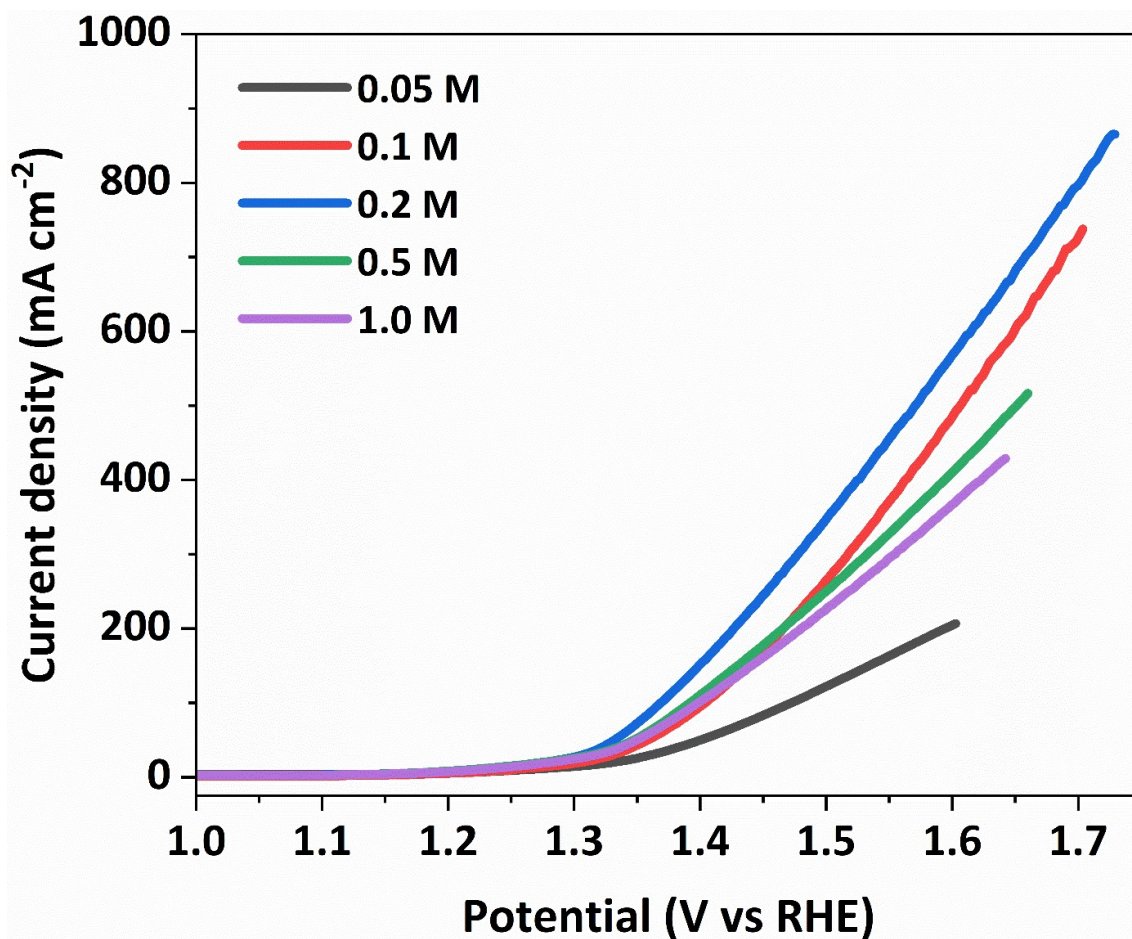


**Fig. S6** Optimization of glycerol concentration in 1 M KOH with anodic oxidation at NiCoMn oxide/NF in three electrode system. The polarization curve shows 0.2 M glycerol as optimum concentration for current system and decrease in current density could be from the increasing non ionic organic component (Glycerol).

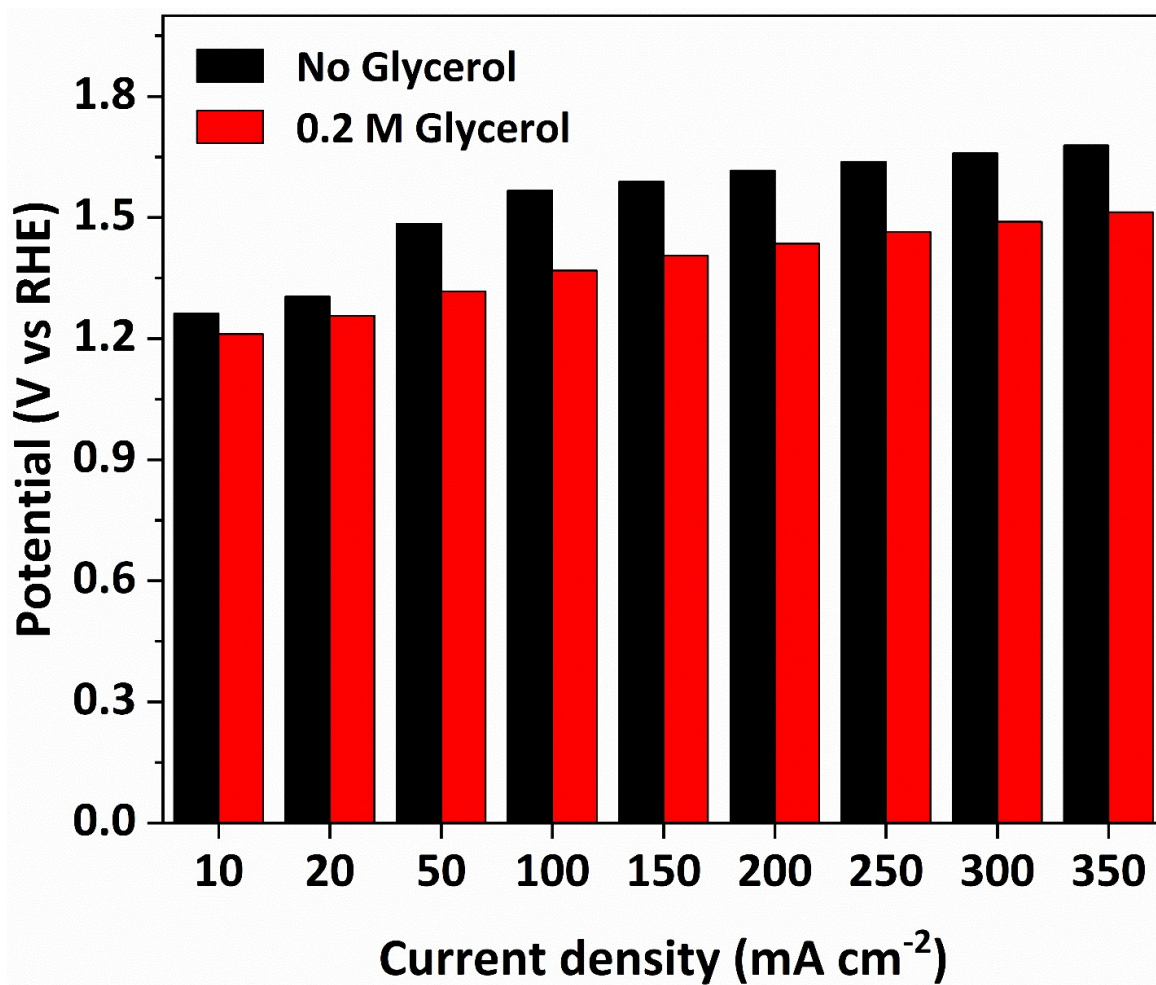
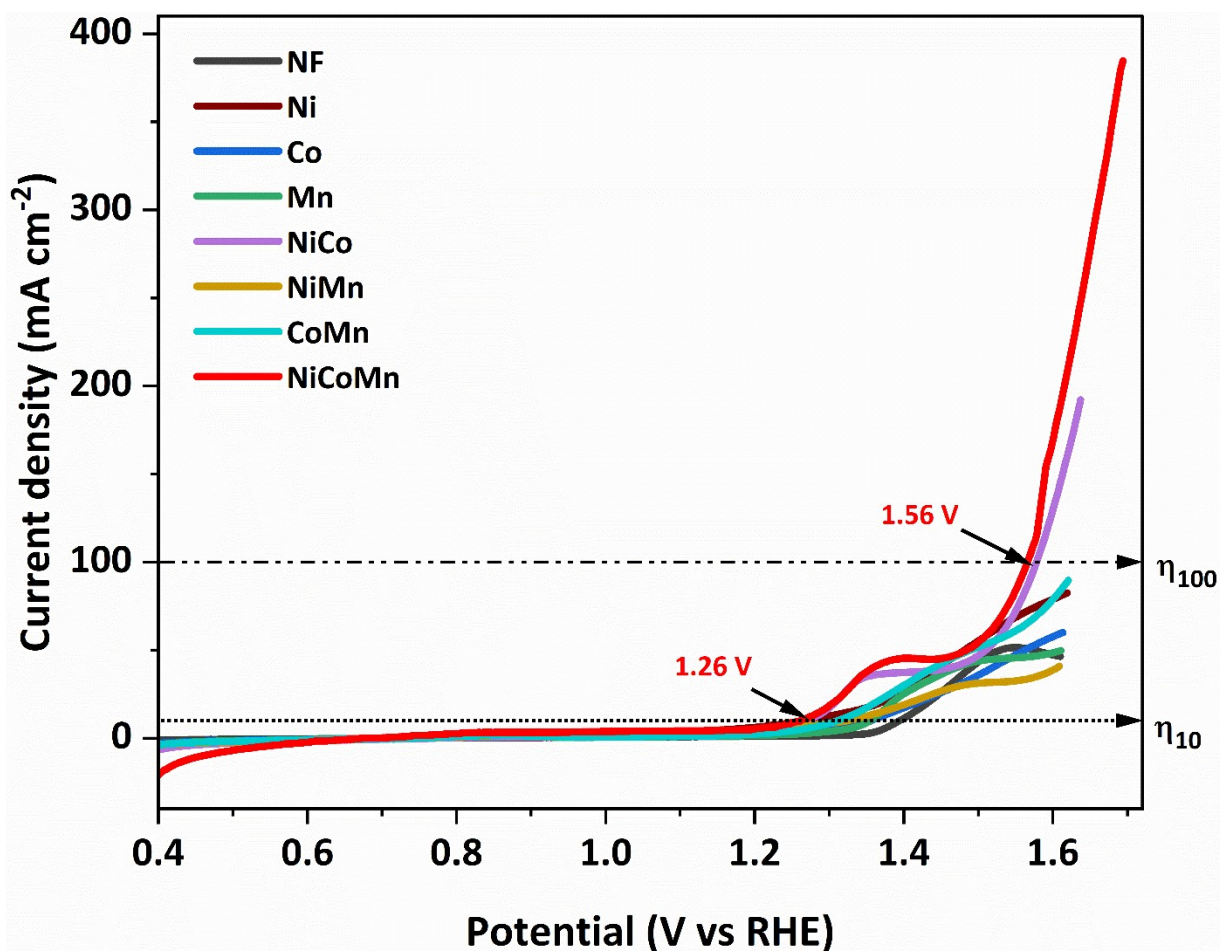
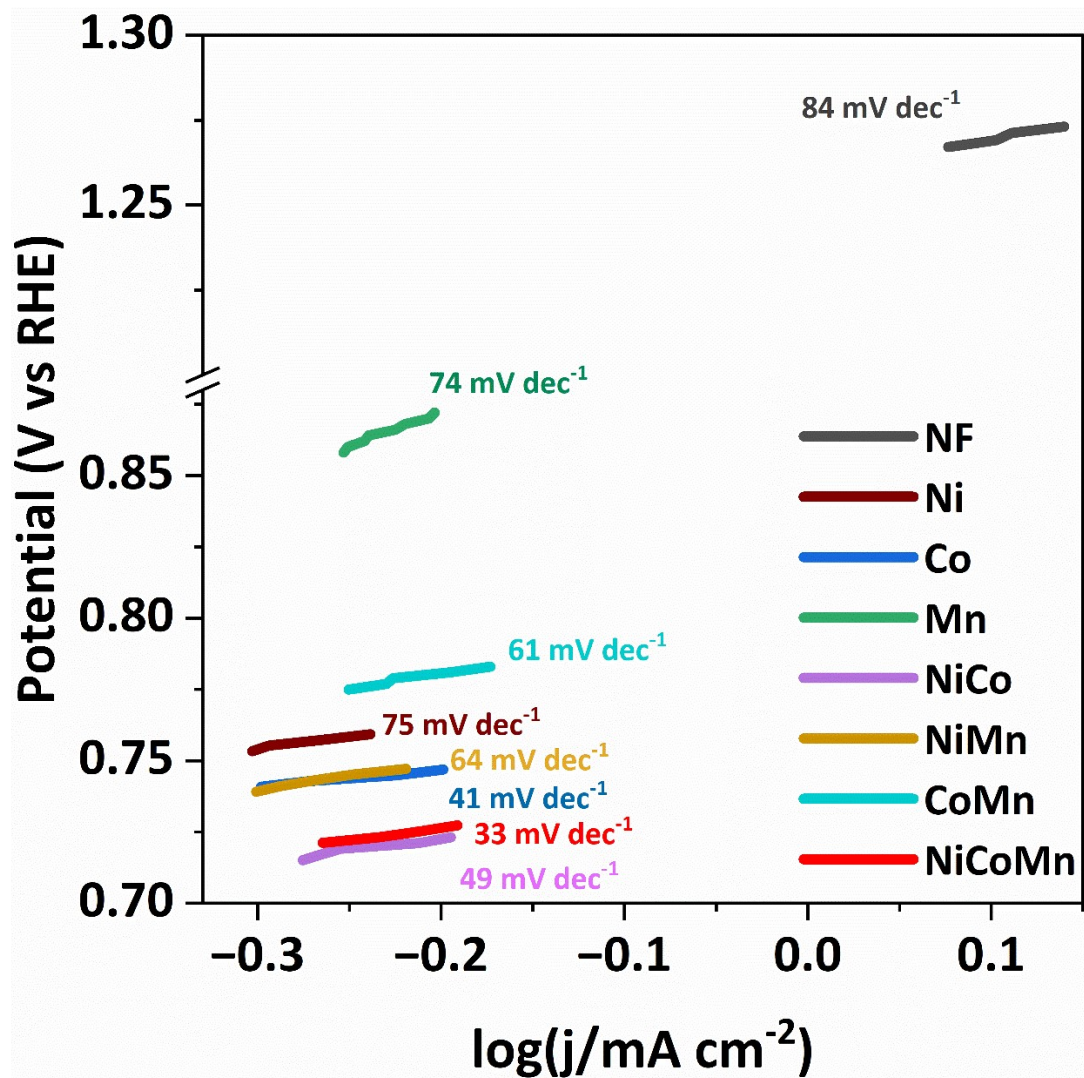


Fig. S7 Comparison of potential needed to attain various current density, with and without glycerol, in 1 M KOH in 3 electrode setup.



**Fig. S8** LSV result observed with NiCoMn/NF anode in 1.0 M KOH . Scan rate: 5 mV s<sup>-1</sup>. The oxidation current predominates with NCMO/NF, water electrolysis has been performed in three electrode system. All other monometallic and bimetallic oxide systems also evaluated and they are all significantly inferior in activity than NCMO.





**Fig. S9** Tafel slope of NCMO, and bimetallic combinations and monometallic counterparts. The NCMO/NF shows the lowest slope among them. The slopes were taken at onset potential.

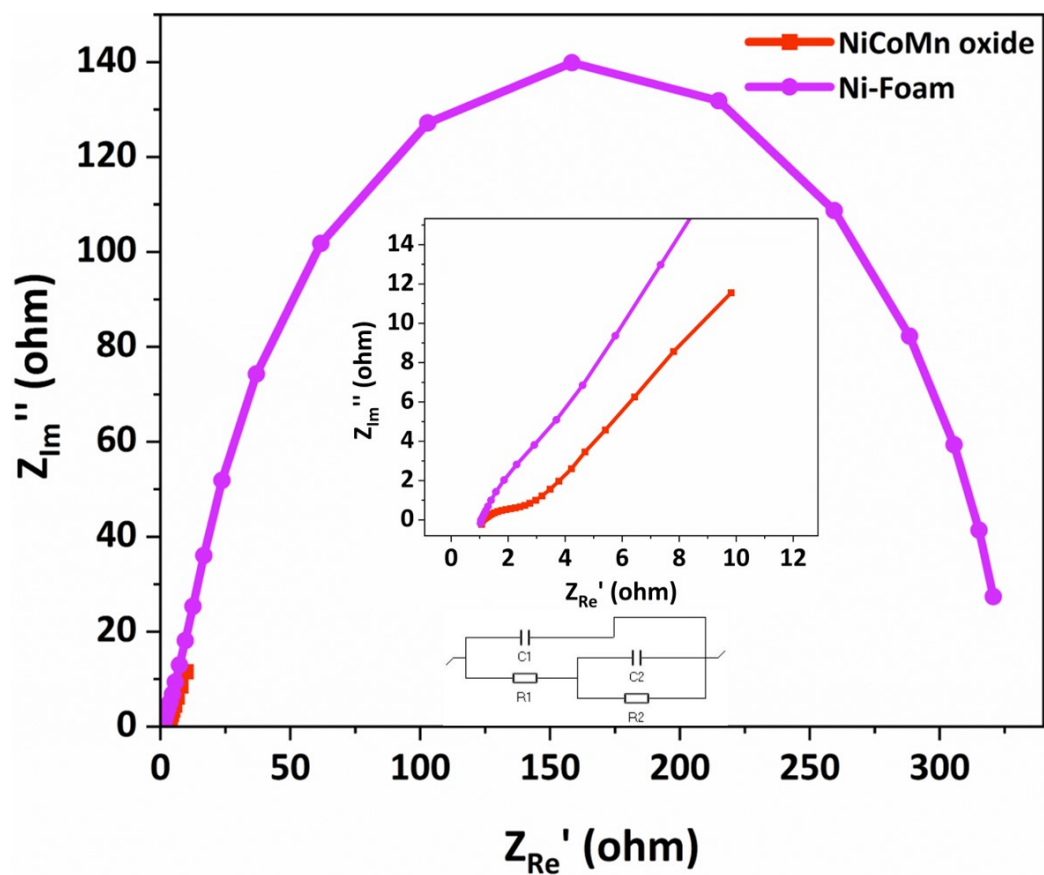


**Fig. S10** The electrochemical impedance spectra, performed at 0.0 V vs  $E_{oc}$  in a 0.2 M gly and 1 M KOH electrolyte. EIS measurements were performed in a frequency range from 25,000 to 0.1 Hz with 10 mV amplitude.

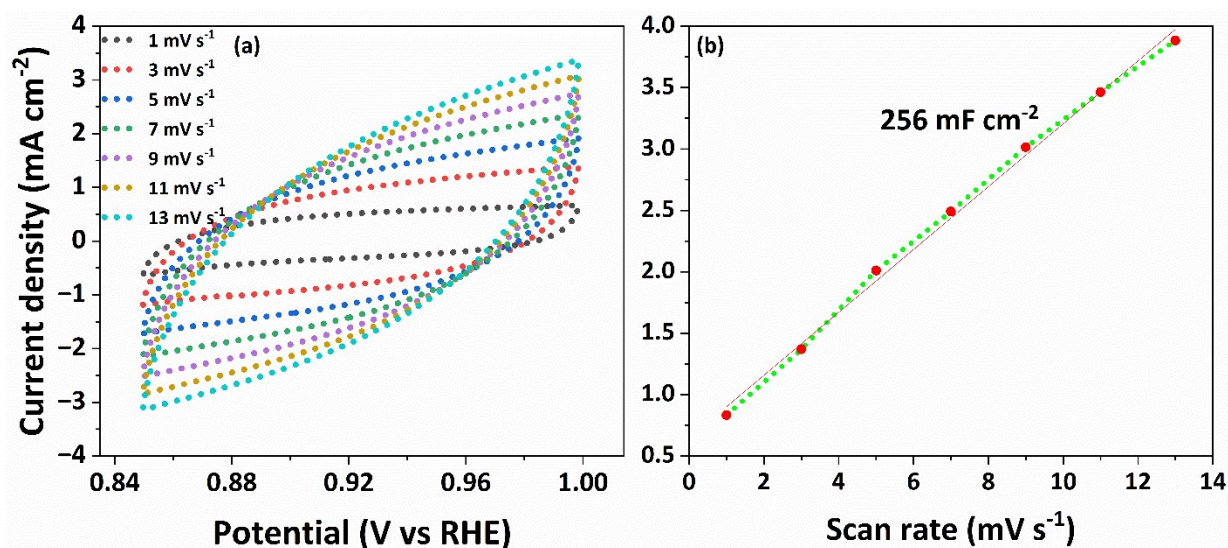


**Fig. S11** (a) The electrochemically active surface area of the produced NCMO catalyst was measured using double-layer capacitance measurements using cyclic voltammetry in 1 M KOH. (A), Cyclic voltammograms were recorded in the non-Faradaic region at the following scan rates: 0.001 ( black line), 0.003 (dark red line), 0.005 (blue line), 0.007 (green line), 0.009 (purple line), 0.011 (daisy yellow line), and 0.013 (cyan line). Before starting the subsequent sweep, the working electrode was maintained at each potential vertex for 30 seconds. It is presumed that capacitive charging is the source of all current. (b) Linear fitting for scan rates to current densities for double layer capacitance of electrochemical surface area (ECSA) of NCMO/NF catalysts, the scanning potential range was from 0.849 V to 0.998 V vs RHE

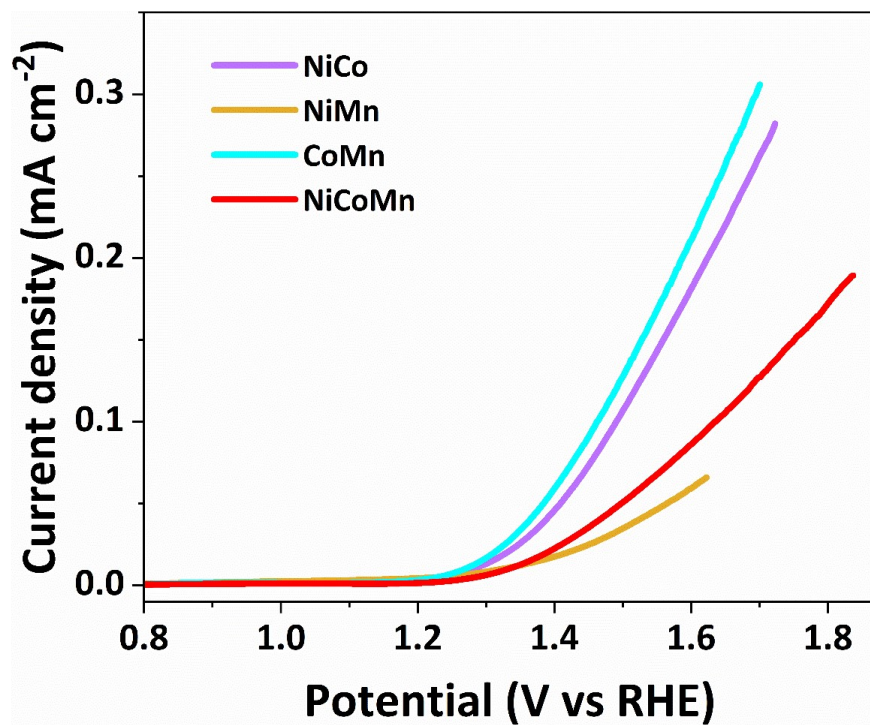
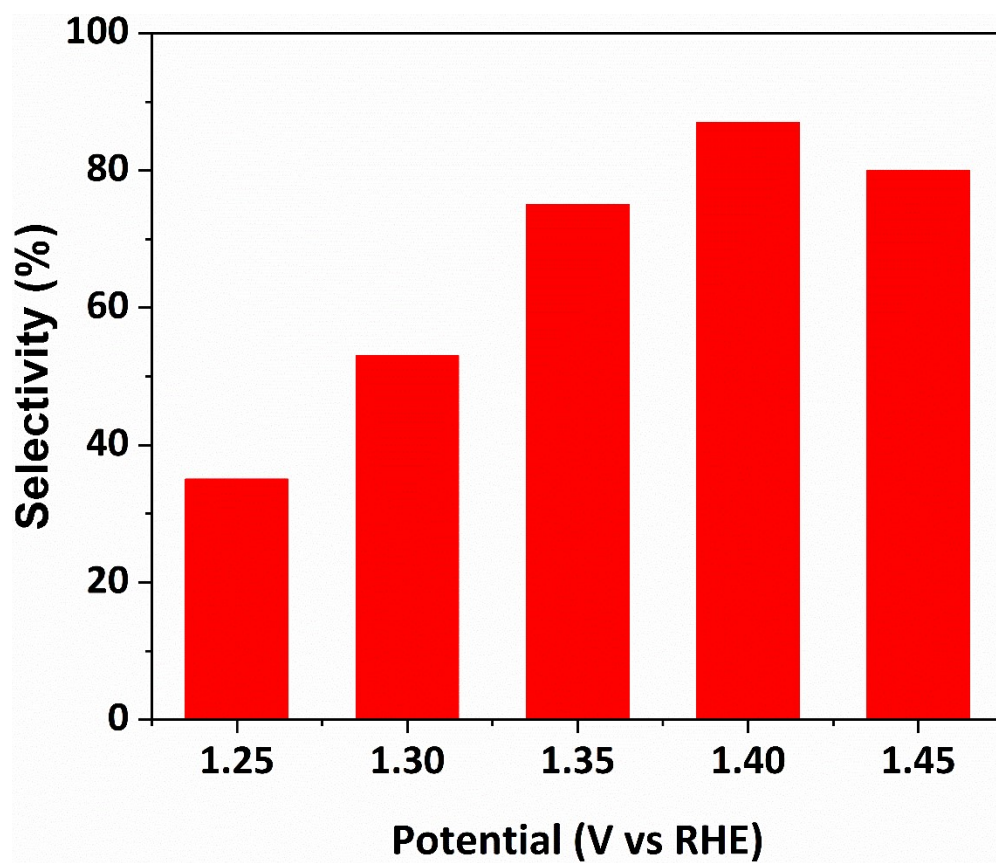
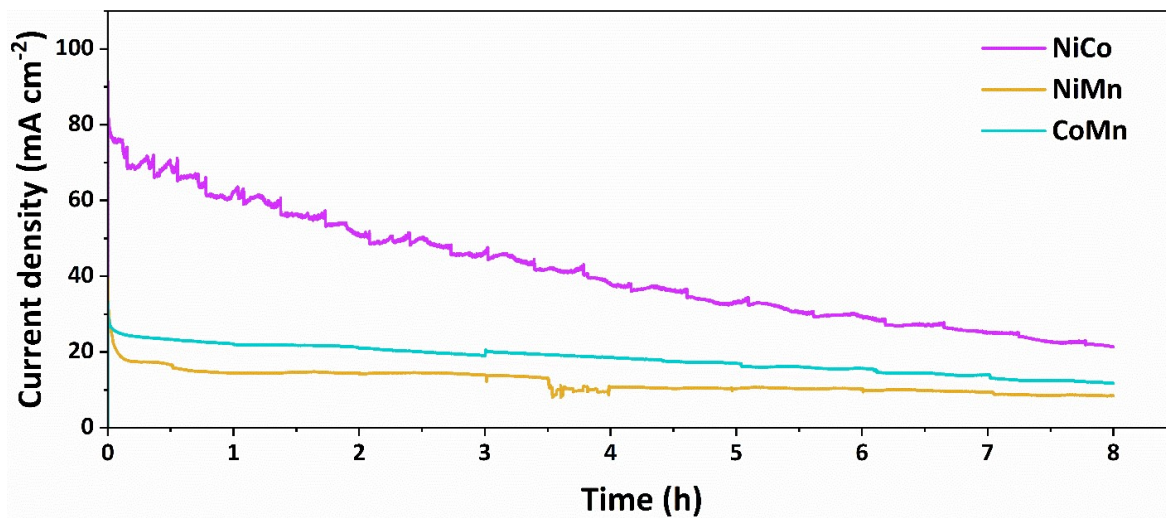


Fig. S12 ECSA normalized LSV polarization curve for Glycerol oxidation reaction





**Fig. S13** Selectivity for formate production at various potentials. (1.45, 1.4, 1.35, 1.3, 1.25 V vs RHE), a certain amount of voltage is required to initiate the C-C cleavage, whereas going higher potentials may introduce overoxidation to  $\text{CO}_3^{2-}$  etc.



**Fig. S14** Chronoamperometry of bimetallic combinations (NiCo, NiMn, CoMn) at cathode in 0.2 M gly . Potential 1.4 V vs RHE. The chronoamperometry product distribution of NiCo/NF is similar, but selectivity decreases for formate. NiMn/NF and CoMn/NF seems less efficient towards glycerol oxidation

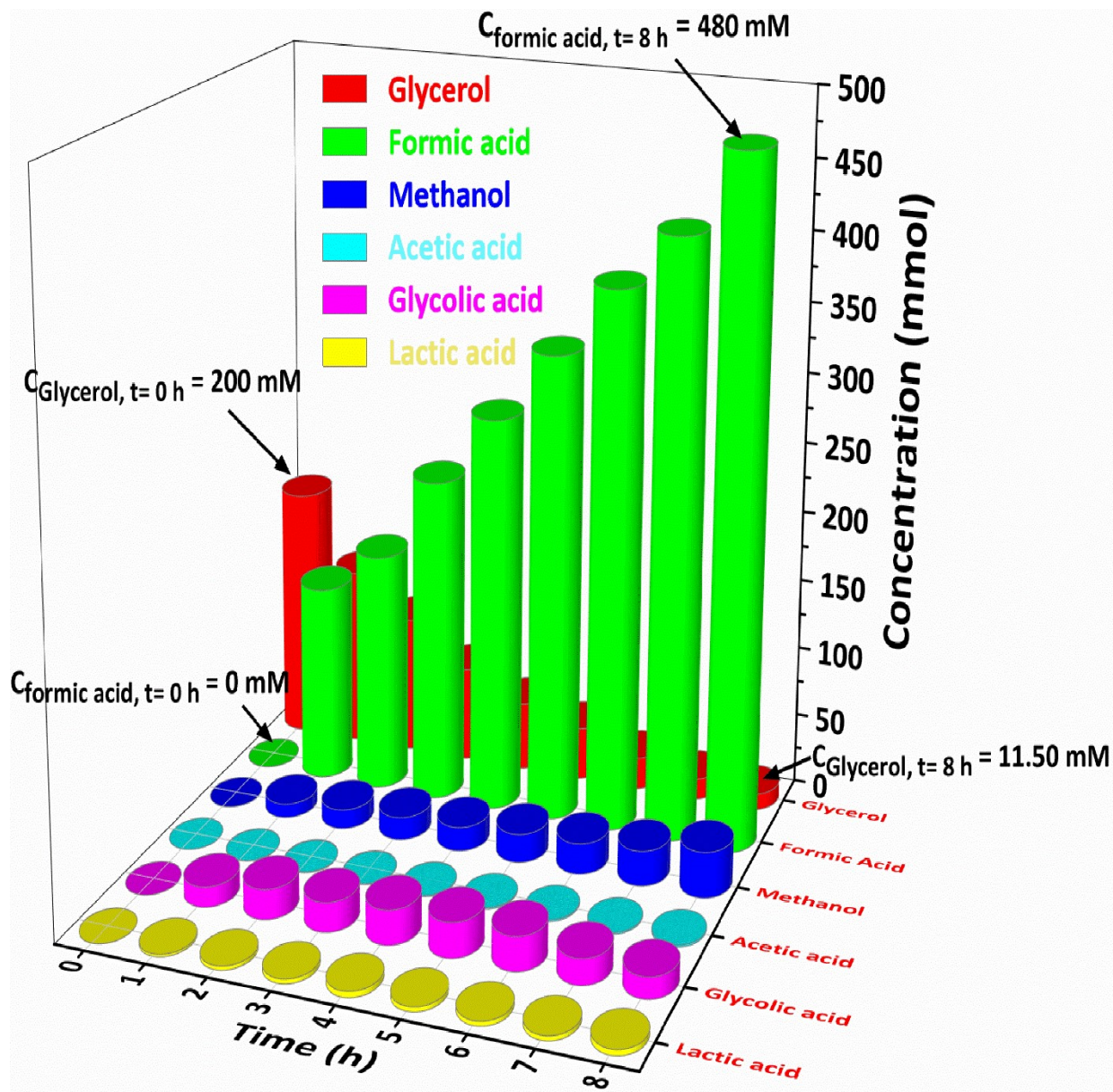


**Fig. S15** Reactant and product distribution observed from the chronoamperometry test carried out at 1.4 V vs RHE for NCMO/NF.

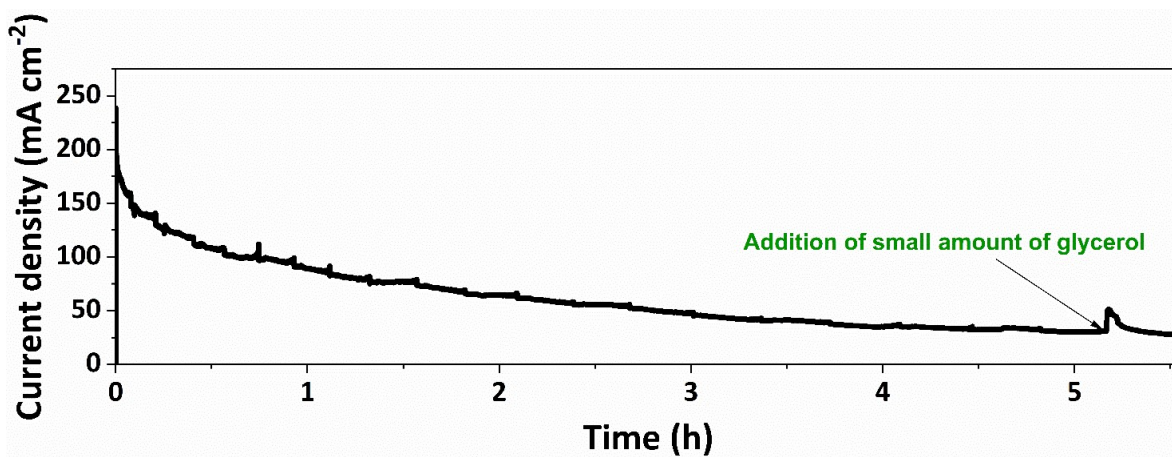


**Fig. S16** Addition of glycerol after significant conversion of glycerol, to find out further addition of Glycerol increases the reaction rate and current density. This also suggests the superiority of Glycerol oxidation over other intermediate.



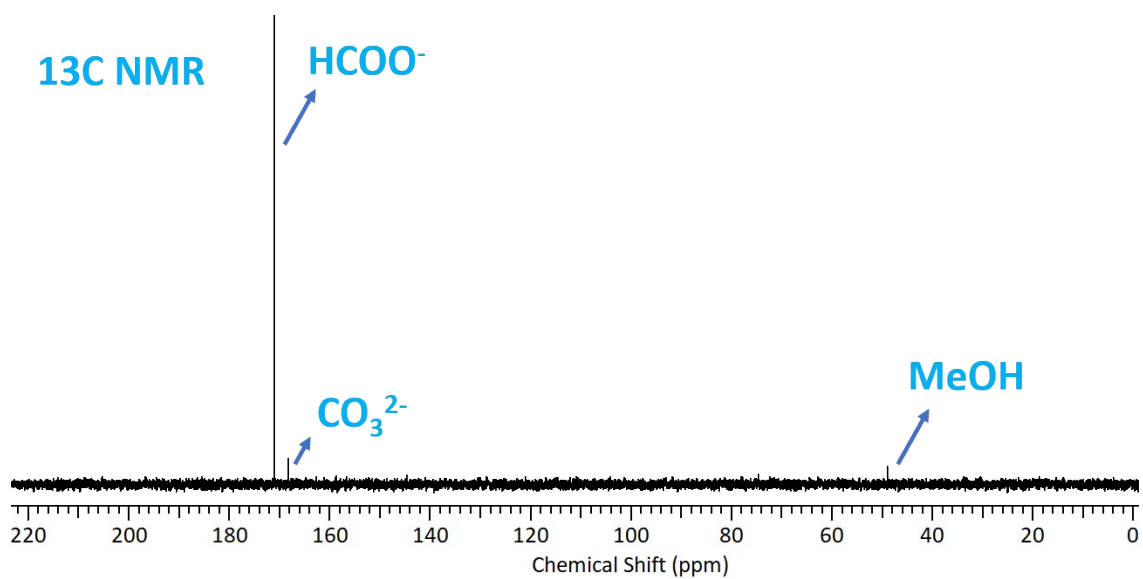


**Fig. S17**  $^{13}\text{C}$  NMR spectroscopy of chronopotentiometry carried out at 1.4 V vs RHE with 0.2 M glycerol with NCMO/NF. A small  $\text{CO}_3^{2-}$  is observed after 8 h of reaction

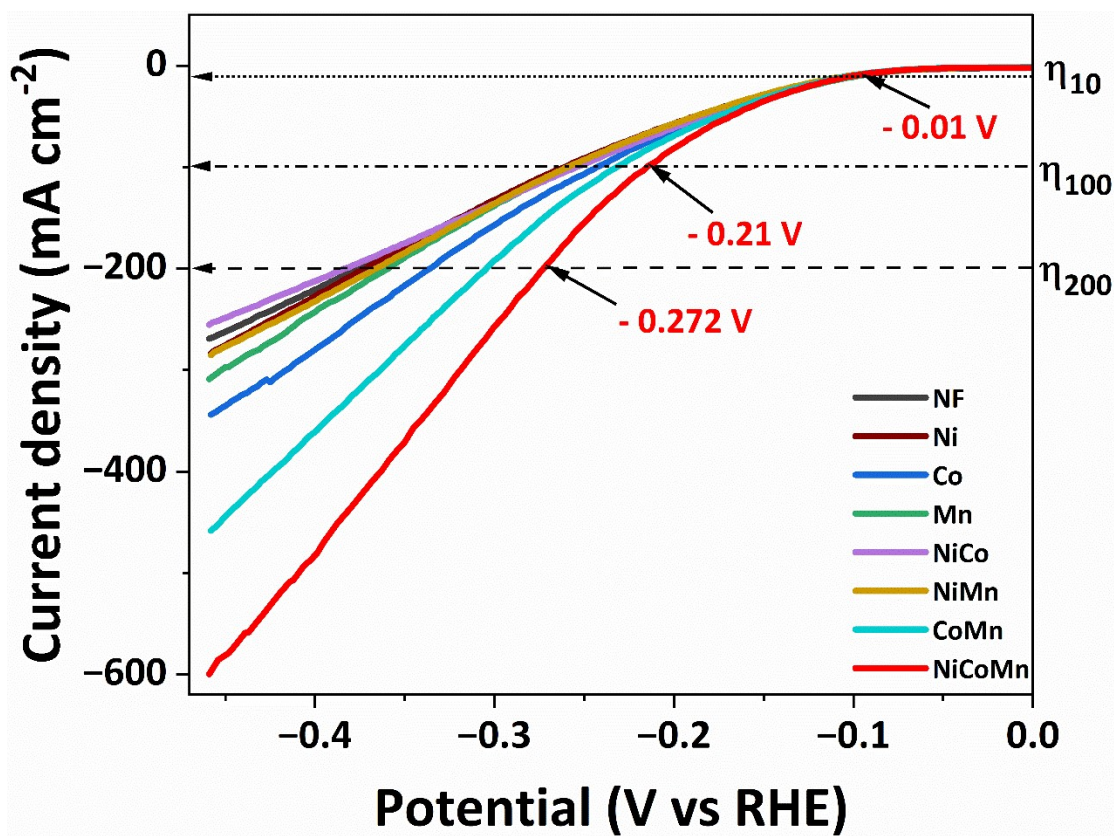


Fig. S18 LSV polarization curves for NCMO/NF (and other monometal and bimetal combinations) as cathode for HER in 0.2 M gly . Scan rate: 5 mVs<sup>-1</sup>

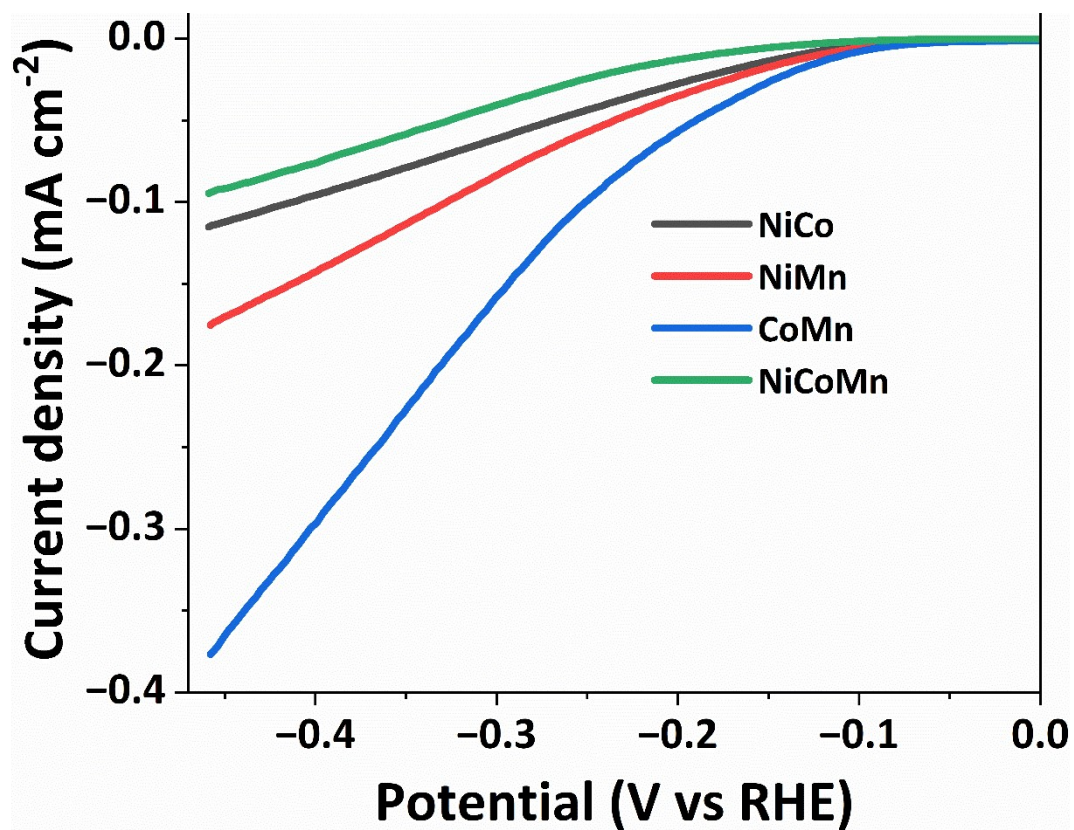
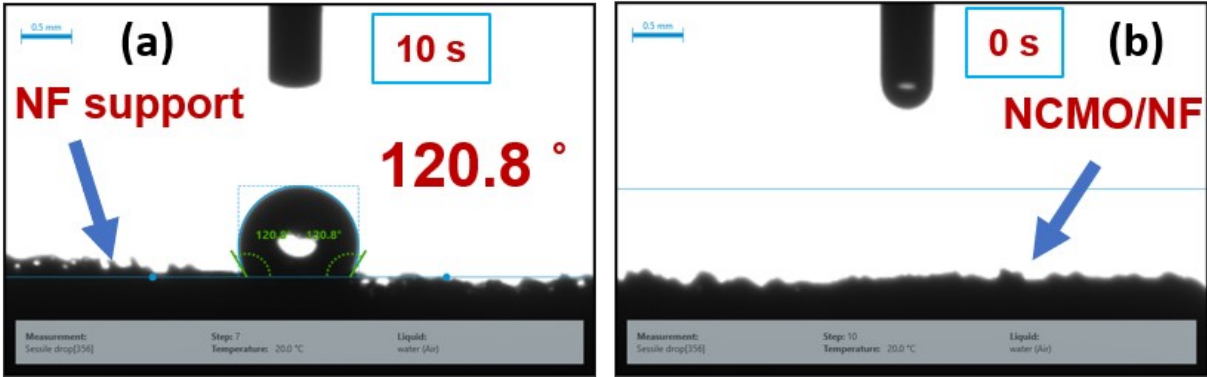
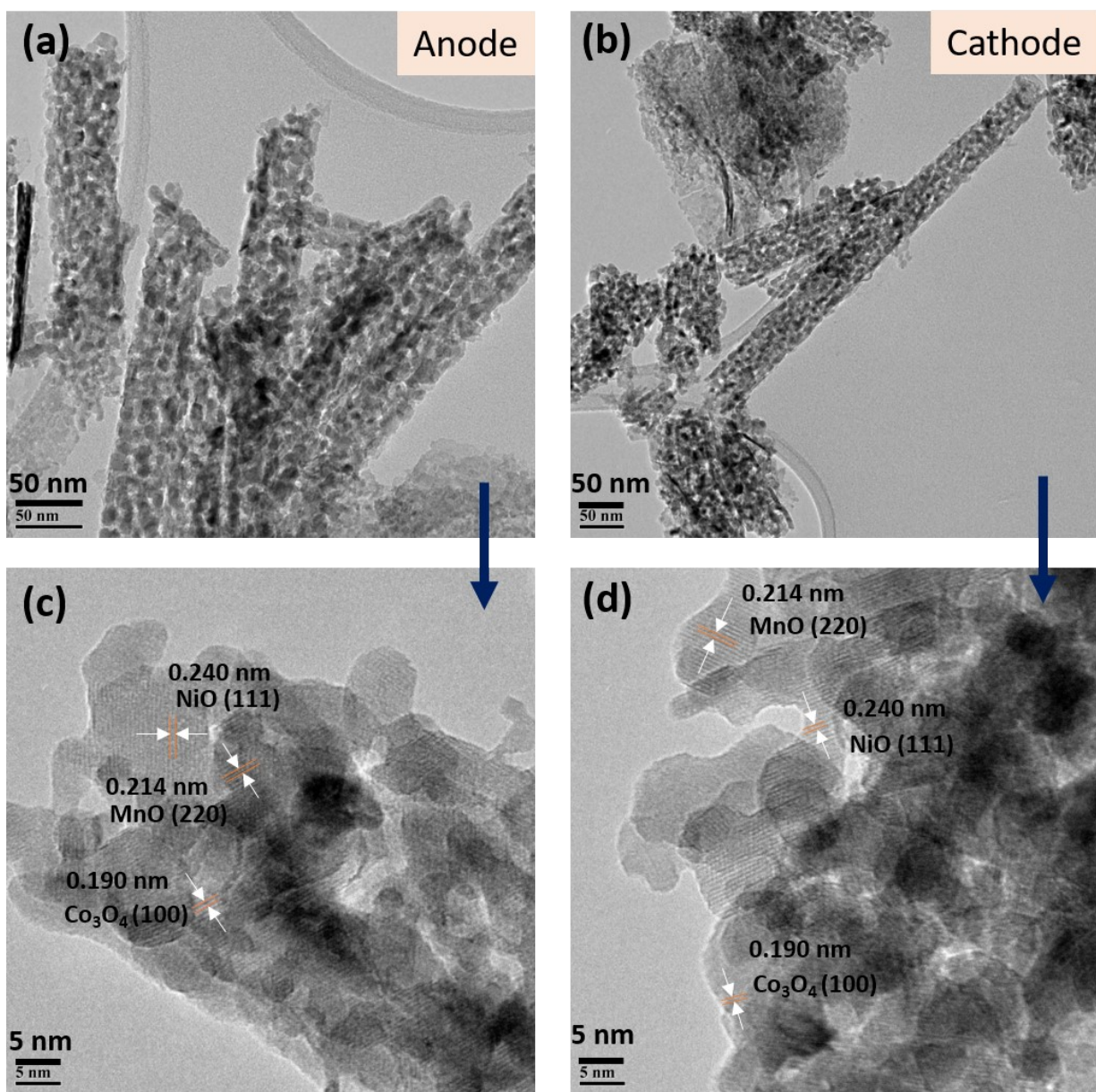


Fig. S19 ECSA normalized polarization curve for the bimetallic and trimetallic catalyst for HER



**Fig. S20** Contact angle measurement made on NF support and NCMO/NF with water. (a) The timescale shows, in NF hydrophobicity maintains after 10s (b) In case of NCMO/NF water gets absorbed by surface immediately after contact, shows superhydrophilicity.

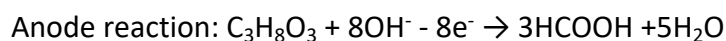




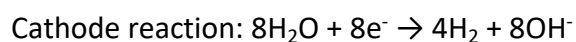
**Fig. S21** TEM images after 120 h of electrolysis of (a,b) anode, cathode shows the nanoneedle appearance after stability test (c,d) The high resolution TEM image shows that the appearance of lattices fringes corresponding to the retained nano crystallinity.

## Supplementary note 1

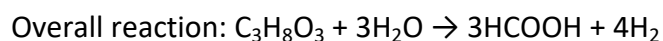
Theoretical Gibb's free energy ( $\Delta G$ ) and potential (E) of reaction for the anodic electro-oxidation of glycerol ( $C_3H_8O_3$ ) to formic acid (HCOOH) coupled to the cathodic HER (Standard molar free energy of formation ( $\Delta G_f$ ):  $C_3H_8O_3$  (l):  $-478.6 \text{ KJ mol}^{-1}$ ,  $H_2O$  (l):  $-237.13 \text{ KJ mol}^{-1}$ ,  $OH^-$  (l):  $-157.244 \text{ KJ mol}^{-1}$ ,  $HCOOH$  (l):  $-361.3 \text{ KJ mol}^{-1}$ ):



$$\Delta G_{\text{Anode reaction}} = -532.998 \text{ KJ mol}^{-1} \quad E_{\text{Anode reaction}} = 0.69 \text{ V}$$



$$\Delta G_{\text{Cathode reaction}} = 639.088 \text{ KJ mol}^{-1} \quad E_{\text{Cathode reaction}} = -0.83 \text{ V}$$



$$\Delta G_{\text{Overall reaction}} = 106.09 \text{ KJ mol}^{-1} \quad E_{\text{Overall reaction}} = -0.137 \text{ V}$$

## Supplementary note 2

$$\text{Conversion (\%)} = \frac{n_{\text{glycerol, initial}} - n_{\text{glycerol, final}}}{n_{\text{glycerol, initial}}}$$

$$\text{Carbon balance (\%)} = \frac{n_{\text{Sum of products}}}{3 \times n_{\text{glycerol, initial}}} \times 100$$

$$\text{Selectivity (\%)} = \frac{n_{\text{product}} \times \text{carbon balance}}{n_{\text{Sum of products}}} \times 100$$